Organic & Biomolecular Chemistry

PAPER

View Article Online
View Journal

Cite this: DOI: 10.1039/c5ob01506e

Synthesis of the cyanobacterial metabolite nostodione A, structural studies and potent antiparasitic activity against *Toxoplasma gondii*†

James McNulty,*[a] Kunal Keskar,[a] Hilary A. Jenkins,[a] Nick H. Werstiuk,[a] Claudia Bordón,[b] Robert Yolken[b] and Lorraine Jones-Brando[b]

Received 21st July 2015,
Accepted 12th August 2015

DOI: 10.1039/c5ob01506e

www.rsc.org/obc

A total synthesis of the cyanobacterial natural product nostodione A is reported involving a convergent, diversity-oriented route, enabling the assembly of a mini-library of structural analogues. The first single crystal X-ray structural determination on a member of this series is reported along with SAR studies identifying potent inhibitors of invasion and replication of the parasitic protozoan *Toxoplasma gondii*.

The isolation of biologically active secondary metabolites from cyanobacteria (blue-green algae) of diverse origin, including from marine, freshwater and terrestrial environments, has proven prolific in terms of structural diversity as well as the wide range of therapeutic potential demonstrated.[1] The indole-containing natural product nostodione A (**1**) (Fig. 1) was first isolated from the terrestrial cyanobacterium *Nostoc commune* in 1994 and shown to inhibit mitotic spindle formation.[2] The same compound was subsequently isolated from the freshwater cyanobacterium *Scytonema hofmanni* and shown to possess proteasome inhibitory activity.[3] Nostodione A exists as a thermodynamic mixture of the (*E*)- and (*Z*)-*conformational* isomers shown (Fig. 1). The compound is believed to be biosynthesized from prenostodione,[4a] an oxidative coupling product of 4-hydroxyphenylpyruvic acid from L-tyrosine and L-tryptophan.[4b] Nostodione A belongs to a family of related alkaloids that have been isolated from cyanobacteria in recent years including the dimer scytonemin (**2**), (Fig. 1).[5] In addition to the anti-mitotic and proteosomal activities described above, these highly UV-absorbing molecules may also serve a protective function against solar radiation within the cyanobacterial colony and are of interest as potential sunblock ingredients. The chemical synthesis of isoprenostodione,[6a] as well as two successful total syntheses of nostodione A (**1**)[6b,f] and a single report on the synthesis of the dimer scytonemin (**2**)[6c] have been reported to date. An enzymatic approach to the scytonemin monomer has also recently been reported,[6d] as has the synthesis and antiproliferative activity of a series of deoxy analogues of nostodione A.[6e]

We became interested in the synthesis and biological evaluation of nostodione A (**1**) for several reasons. Our research groups recently initiated a joint program aimed at the discovery of novel small-molecules exhibiting biological activity against the parasite *Toxoplasma gondii*, Fig. 1, the protozoan responsible for toxoplasmosis, a cause of severe systemic and neurological disease in neonates and immune compromised individuals.[7] From a structural viewpoint, nostodione A resembles several known oxidized, condensed indole alkaloids such as indirubin, tryptanthrin[8] and the pyrroloiminoquinones,[9] examples of which display activity against *T. gondii*. We recently communicated the successful total synthesis of **1** *via* a late stage, diversity oriented strategy.[6f] Synthetic access to nostodione A and analogues indeed allowed identification of activity towards *T. gondii*. In this full paper we report the full development and extension on this successful late-stage, diversity-oriented synthetic approach towards nostodione A and analogues, theoretical and X-ray structural studies and details on the potent biological activity of these derivatives to *T. gondii*.

Two retrosynthetic possibilites with which to access nostodione A (**1**) were considered, as outlined in Fig. 2. In both potential routes, in order to conduct structure–activity evaluation of analogues of (**1**), we considered that either a Horner–Wadsworth–Emmons (HWE)-type or Wittig-type disconnection of the 4-hydroxystyryl unit in (**1**), leading to the β-ketophoshonate (**3a**) or phosphonium salt (**3b**) and 4-hydroxybenzaldehyde, or protected derivative thereof (ArCHO), would be most versatile. In the synthetic direction, the β-ketophosphonate

[a]*Department of Chemistry and Chemical Biology, McMaster University, Hamilton, Ontario, Canada, L8S 4M1. E-mail: jmcnult@mcmaster.ca; Fax: (+1)-905-5222509; Tel: (+1)-905-525-9140 Ext. 27393*

[b]*Stanley Division of Developmental Neurovirology, Department of Pediatrics, Johns Hopkins University School of Medicine, 600 North Wolfe Street, Baltimore, Maryland 21287, USA*

†Electronic supplementary information (ESI) available: Synthetic procedures and characterisation data for all new compounds. CCDC 1051478. For ESI and crystallographic data in CIF or other electronic format see DOI: 10.1039/c5ob01506e

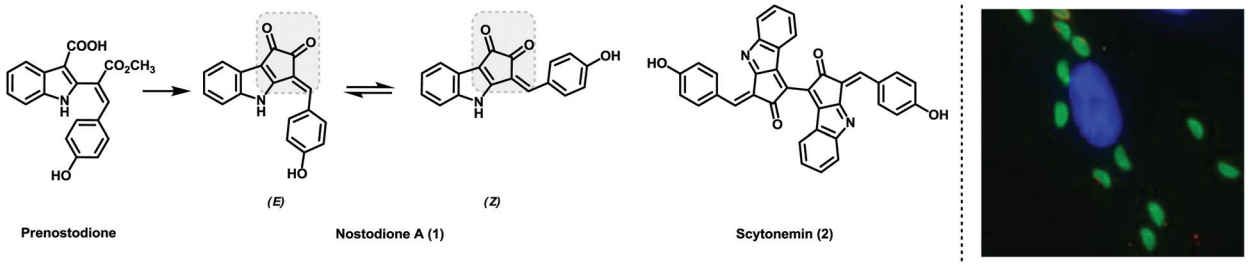

Fig. 1 The cyanobacteria-derived natural product nostodione A (**1**), related alkaloids. Crescent shaped *Toxoplasma gondii* tachyzoites (green) inside human fibroblast host cells (nucleus in blue).

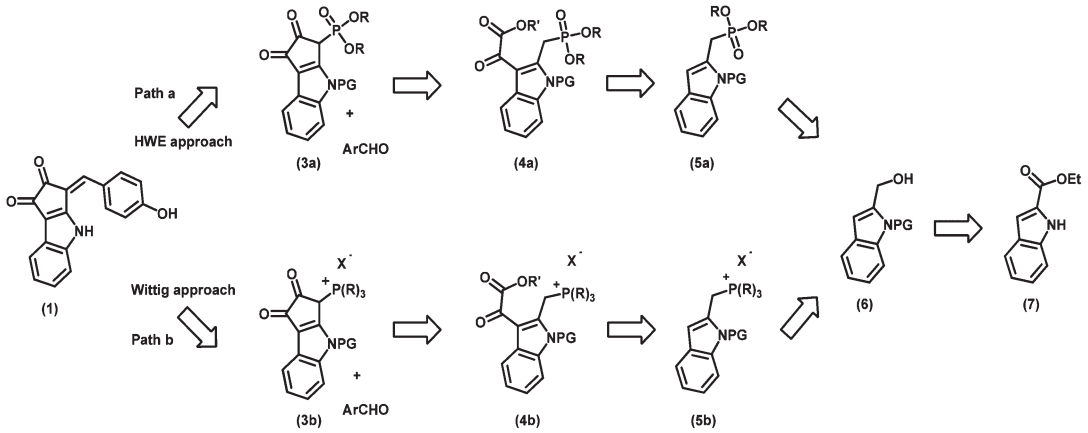

Fig. 2 Retrosynthetic analyses considered of nostodione A (**1**) designed to introduce late-stage structural diversity.

(**3a**) or phosphonium salt (**3b**) were envisioned as an ideal nexus that would allow construction of an assemblage of nostodione A analogues *via* a late-stage, diversity-oriented olefination reaction (with ArCHO or RCHO) in the last step. It was envisioned that the β-ketophosphonate (**3a**) or salt (**3b**) would be accessible through either an intramolecular α-phosphonate acylation-type reaction[10] or phosphonium acylation, from the 3-oxalylindole derivatives (**4a,b**), in turn, the product of acylation of the indole (**5a,b**) with oxalyl chloride. Compounds (**5a,b**) were projected to be the products of either phosphine quaternization or Michaelis–Arbuzov reaction of a 2-halomethylindole derivative from (**6**), ultimately derived from commercially available indole-2-carboxylic acid derivative (**7**).

We initially began the synthesis following the Wittig-type disconnection (Path b) shown in Fig. 2, beginning with commercially available ethyl-indole-2-carboxylate (**7**), as shown in Scheme 1. In exploratory studies (not shown) we determined that formation of the necessary 2-halomethyindole derivatives was complicated by the presence of the free indole NH. Protection as the *N*-tosyl derivative (**8**) followed by reduction of the ester led efficiently to the desired alcohol (**9**). Conversion to the chloromethyl derivative (**10**) now occurred smoothly and

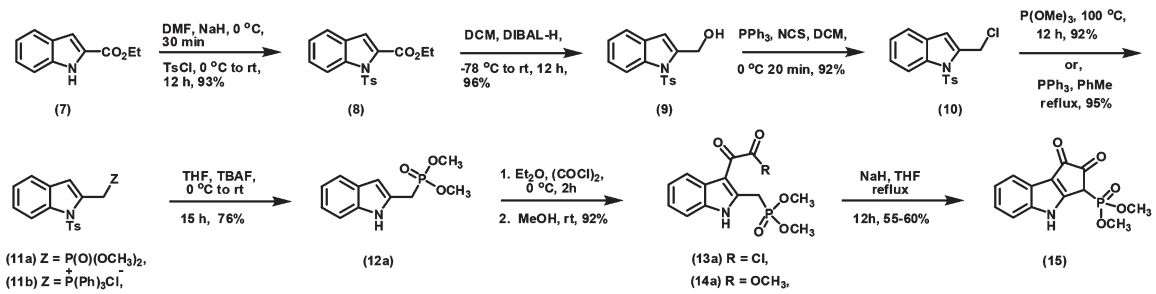

Scheme 1 Synthesis of the 3-oxalyl-indole-2-phosphonomethyl intermediates (**13a**) and (**14a**).

Table 1 Optimisation of the intramolecular phosphonate acylation

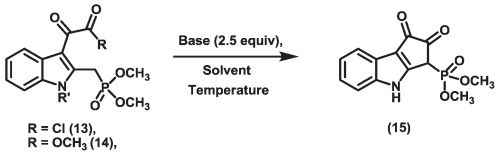

Entry	R/R′	Base	Solvent	Temperature (°C)	Isolated yield (%)
1	–Cl/H	LHMDS	THF	rt	Not clean
2	–Cl/H	NaH	THF	rt	Not clean
3	$-OCH_3$/H	LHMDS	THF	Reflux	38
4	$-OCH_3$/H	LDA	THF	Reflux	Not clean
5	$-OCH_3$/H	KO^tBu	THF	Reflux	22
6	$-OCH_3$/H	NaH	THF	Reflux	55–60
7	$-OCH_3$/H	NaH	PhMe	Reflux	NR
8	$-OCH_3$/H	NaH	THF + HMPA(1 : 1)	rt/reflux	NR
9	$-OCH_3$/H	NaH	THF + DMF(1 : 1)	rt/reflux	Trace
10	$-OCH_3$/PMB	NaH/LHMDS/KO^tBu	THF/DMF	rt/reflux	NR

this reactive intermediate was quaternized with triphenylphosphine giving the *N*-tosyltriphenylphosphonium salt (**11b**) corresponding to (**5b**). The direct *C*3-acylation of this salt proved problematic, most likely due to electronic deactivation at C3 induced by the *N*-tosyl substituent. While removal of the *N*-tosyl group from this intermediate could readily be accomplished using TBAF,[11] this resulted in intractable purification issues and resulted ultimately our abandonment of the Wittig approach as described (Fig. 2).

Returning to the HWE route, the chloromethyl derivative (**10**) underwent clean Michaelis-Arbuzov alkylation with trimethylphosphite yielding phosphonate (**11a**). Direct attempts at *C*3-acylation on intermediate (**11a**) with oxalyl chloride also met with failure, again attributed to *N*-tosyl-induced electronic deactivation at this position. Removal of the *N*-tosyl substituent was accomplished under mild conditions using TBAF and the desired phosphonate (**12**) could be obtained cleanly.[11] Acylation on the deprotected phosphonate (**12**) now occurred smoothly with oxalyl chloride in diethyl ether yielding initially the monoacyl chloride derivative (**13**). Attempts at intramolecular acylation initially proved extremely challenging and a summary of select examples en-route to optimisation of this reaction is collected in Table 1. Attempted intramolecular acylation on the immediate acid chloride (**13**) proved futile with a number of bases and solvents (entries 1 and 2). The acid chloride was converted to the methyl ester (**14**) in order to probe the intramolecular ester acylation.[10] A wide range of conditions were investigated for the conversion of (**14**) into the β-ketophosphonate (**15**). The use of sodium hydride (NaH) in refluxing THF proved optimal and compound (**15**) could be isolated in reasonable yields of 55–60%. We also attempted to convert the acid chloride to its corresponding 2,2,2-trifluorethyl ester, however the product isolated proved to be the decarbonylated indole-3-carboxylate trifluoroethyl ester. With the β-ketophosphonate (**15**) now on hand, we began initial studies on the critical HWE reaction as summarized in Scheme 2. Protection

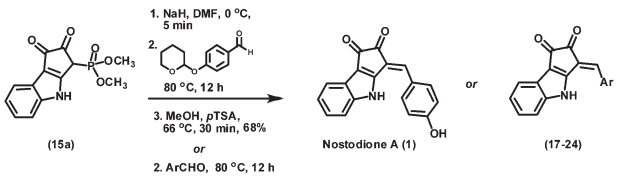

Scheme 2 Completion of the synthesis of nostodione A (**1**) and analogues employing the HWE strategy.

of 4-hydroxybenzaldehyde with dihydropyran gave the unstable 4-tetrahydropyranyl ether. This was reacted with the dianion generated from (**15**) and the HWE reaction proceeded smoothly to give the THP-protected derivative of nostodione A (**16**) which was immediately deprotected, completing the synthesis of nostodione A in 68% isolated yield from (**15**). Synthetic nostodione A was isolated as a yellow pigment with m. p. 285 °C (decomp), lit. mp 280 °C (decomp)[2] and spectroscopic data in accord with the literature values including an (*E*) : (*Z*) ratio of 4 : 1 (acetone) for both our synthetic material and the natural product.[2,6c] This synthesis constitutes the second reported total synthesis of nostodione A and was achieved in only 8 chemical steps and 21.6% overall yield from commercial ethyl indole-2-carboxylate (**7**).

The structure of nostodione A (**1**) was initially deduced from extensive spectroscopic analysis on the natural product,[2,3] as well as degradations studies on the dimer,[5] and has now been confirmed by two independent total syntheses.[6b,f] Nonetheless, the nature of the fused cyclopentenedione ring system is intriguing and we considered the role of the tautomer or hydrate (Fig. 3) as being possible contributors to the obvious stability of the molecule. No X-ray analysis has so far been reported on any nostodione A derivative. Nonetheless, after many recrystallization attempts, we succeeded in obtaining crystals of nostodione A methyl ether **19**[12a] that

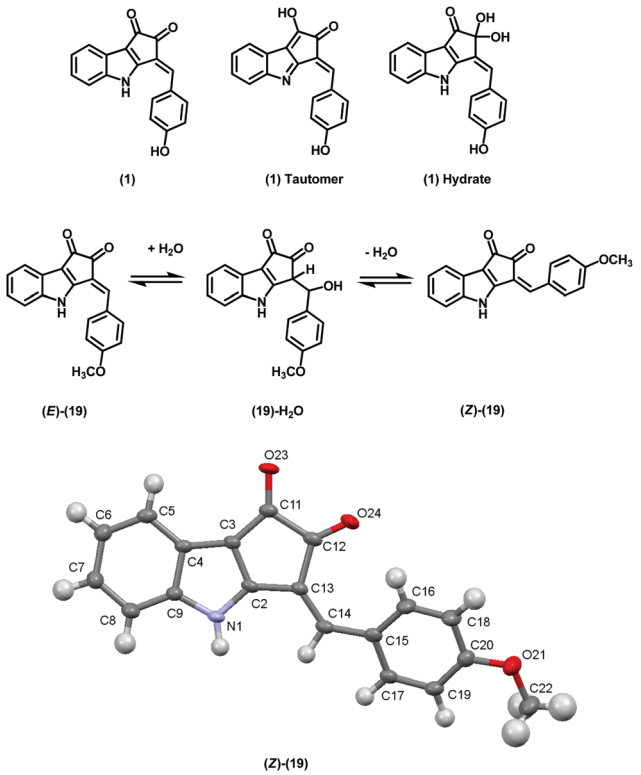

Fig. 3 ORTEP diagram of (*Z*)-(**19**), with non-hydrogen atoms shown at 50% probability.

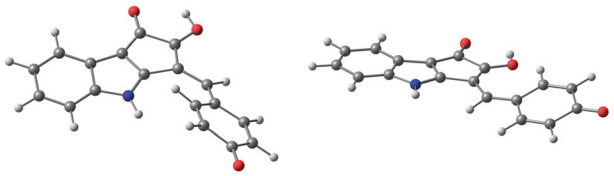

Fig. 4 Calculated structures for the (*E*)- and (*Z*)-quinoid tautomers of nostidione A.

proved suitable for such analysis. Single crystals of (**19**) were slowly deposited from DMSO, and the resulting structure is shown below (Fig. 3). Nostodione A methyl ether was proven to have the correct overall connectivity as expected. Other notable features include the presence of an extended H-bond network between the indolyl NH of one molecule and C11 carbonyl oxygen, corresponding to the tautomer shown (Fig. 3). Several unusually long sp^2–sp^2 bonds are found in the cyclopentane ring (C11–C12, 1.54 Å; C12–C13, 1.51 Å) and interestingly, the 4-methoxyaryl ring is tilted approximately 22.8° in relation to the plane of the tricylic-indolyl core. Most intriguingly was the observation that the thermodynamically less stable isomer (*Z*)-**19** deposited selectively from DMSO. Nostodione A methyl ether (**19**) was observed in solution by NMR (DMSO) as a 94 (*E*) : 6 (*Z*) mixture of isomers. DFT optimizations[12b] of the (*E*): and (*Z*) nostodione methyl ethers at the B3PW91/6-31+G(d,p) level showed the (*E*)-isomer to be 1.36 kcal mol^{-1} ($\Delta(E_{Total} + ZPE_{corr})$) more stable than the (*Z*)-isomer. This result indicates that the NMR-observed ratio of isomers corresponds approximately to the computed difference in ground state energies, strong evidence that the isomers are rapidly interconverting in solution. DFT optimizations[12b] and frequency calculations of the (*E*)- and (*Z*)-nostodiones (free phenol) at the B3PW91/6-31+G(d,p) level also showed the (*E*)-isomer to be 1.40 kcal mol^{-1} $\Delta(E_{Total} + ZPE_{corr})$ more stable than the (*Z*)-isomer. The mechanism responsible for the (*E*)- to (*Z*)-isomerization in these nostodione derivatives is unknown, we were unable to obtain a transition state structure for the direct transformation. While dipolar resonance structures may be considered for (*E*)-**19**, lowering the potential barrier to a direct isomerization, the X-ray structure confirms strong double bond character between C13 and C14 (1.36 Å, calculated 1.37 Å) and the non-planarity of the 4-methoxyaryl substituent appear to rule out this possibility. Another possibility considered was isomerization proceeding through the quinone tautomer shown (Fig. 4). Calculations[12b] were thus carried out on the isomeric (*E*)- and (*Z*)-quinoids at the B3PW91/6-31+G(d,p) level. The (*E*)-quinoid was found to be 19.72 kcal mol^{-1} ($\Delta(E_{Total} + ZPE_{corr})$) higher in energy than (*E*)-nostodione A: the (*Z*)-quinoid was 19.94 kcal mol^{-1} ($\Delta(E_{Total} + ZPE_{corr})$) higher in energy than (*Z*)-nostodione A (Fig. 4), indicating this pathway to be unlikely. The most probable mechanism for isomerization may be *via* the reversible addition of water, as shown in Fig. 3.

With nostodione A itself and the mini-panel of synthetic analogues available, we have now further assessed their anti-protozoal activity.[6f] Potential anti-Toxoplasma and anti-host cell properties of the nostodione mini-library were investigated using an established colorimetric assay[15a] for growth inhibition. Briefly, compounds were added to human foreskin fibroblast (HFF; ATCC) host cells growing in 96-well tissue culture plates and then serially diluted across the plate, resulting in a test range of 320–0.032 μM. *T. gondii* RH-2F tachyzoites (ATCC) that constitutively express β-galactosidase (β-gal) were then added to most wells, leaving 2 wells in each column parasite-free for cytotoxicity testing. After 4 days incubation the substrate for β-gal, chlorophenol red-β-D-galactopyranoside (CPRG), was added to the Toxoplasma wells. Further incubation for 20 h was followed by addition of the cell viability reagent, CellTiter 96 Aqueous One Solution Reagent (Promega Corp., WI) to the parasite-free wells. Color reactions were read in a Vmax microplate reader (Molecular Devices, CA) The amount of absorbance in wells containing drug, Toxoplasma, and CPRG was compared to that in drug-free parasite control wells. In the cytotoxicity wells, the extent of bioreduction of the cell viability reagent into a soluble, colored formazan product, a direct indicator of viability, was determined by absorbance in drug-treated *versus* drug-free wells. The median and 90% inhibitory concentrations (IC_{50}, IC_{90} respectively) and the median cytotoxic dose (TD_{50}) were calculated using CalcuSyn software (Biosoft, Cambridge, U.K.). For each compound, a therapeutic index (TI) was calculated with the formula

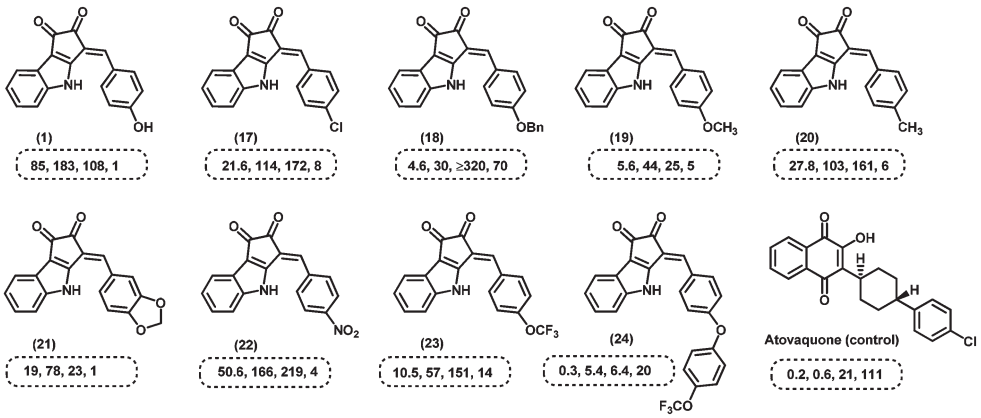

Fig. 5 Nostodione A (**1**) and mini-panel (**17**)–(**24**) prepared *via* the HWG strategy and anti-Toxoplasma activity. Activity reported above are in μM and in following order IC_{50}, IC_{90}, TD_{50}, TI.

TI = TD_{50}/IC_{50}. This number reflects the specific activity of a compound against Toxoplasma. Atovaquone, an anti-parasitic drug used therapeutically to treat many parasitic protozoan diseases including malaria as well as toxoplasmosis, was used as the assay positive control. The tachyzoite and host cell inhibitory activity data are summarized in Fig. 5.

As reported previously,[6f] nostodione A (**1**) exhibited low efficacy against *in vitro T. gondii* with an IC_{50} of 85 μM and a TI of 1. These initial results clearly pointed to the 4-benzyloxy substituent as a key fragment on the anti-toxoplasmosis pharmacophore of nostodione A amenable to further optimisation of both potency and selectivity. The increased activity observed for the two 4-aryl ether derivatives **18** and **19** in connection with potent antimalarial[13a,b] and antitoxoplasmosis[13c] activity reported on endochin-related trifluoromethoxy-substituted aryl ethers prompted our investigation of such derivatives in the nostodione series. The necessary 4-trifluoromethoxyaryloxy benzaldehyde[14] was prepared *via* Cu-mediated cross-coupling of 4-bromobenzaldehyde and trifluoromethoxyphenol, while trifluoromethoxybenzaldehyde itself is commercially available. Further exploitation of the diversity-oriented HWE reaction from (**15**) as described above with these 4-substituted aldehydes allowed synthetic access to trifluoromethoxy analogs (**23**) and (**24**). While the trifluoromethoxy derivative (**23**) proved to be relatively non-cytotoxic (TD_{50} = 151 μM) and no more active (IC_{50} = 10.5 μM) than **18** or **19**, the diaryl ether (**24**) proved to be the most potent derivative thus far discovered in the series, exhibiting an IC_{50} of 300 nM, 280 times as potent as natural nostodione A. The full structure–activity data set is summarised in Fig. 5. As shown, although (**24**) achieved the lowest IC_{50} value, 0.3 μM, the TI, *i.e.*, the specific activity, of this compound was moderated (TI = 20) due to a high level of cytotoxicity (TD_{50} = 6.4 μM). In contrast the previous iterations, 4-benzyloxy-**18** and 4-methoxy-**19** derivatives, exhibited IC_{50} values approximately 1 $\log_{10}$ higher than that of **24**. Further, the 4-methyl- and 3,4-methylenedioxy derivatives were less potent, as were those containing electron withdrawing groups 4-chloro- and 4-nitro (**20**, **21**, **17**, **22**, respectively). The results show clearly that the substituent effect on biological activity is not a simple electronic effect, demonstrating no discernible quantitative structure–activity correlation.

An evaluation of the direct effects of the compounds on extracellular tachyzoites was performed using a standard red/green invasion assay.[15b] This assay evaluates compounds for inhibition of parasite invasion, a process that involves first attachment to host cells and then penetration into the cell by the tachyzoites; immunofluorescent labels distinguish tachyzoites that have actively invaded (green bars) the cells from those that have attached to but are unable to enter (red bars) the cells. A decrease in the number of invaded parasites relative to same of the vehicle [DMSO (VHL)] is indicative of inhibition of parasite invasion, *i.e.* penetration, of the cell whereas a difference in the sum of both invaded and attached parasites (Fig. 6, green + red bars) relative to same of the vehicle indicates an effect on tachyzoite attachment to host cells.[15b] In our preliminary communication,[6f] we reported that all of the earlier derivatives (**1**, **17**–**22**) significantly inhibited tachyzoite invasion of the host cell at 20 μM concentration. Further, all of those compounds significantly inhibited tachyzoite attachment except the 4-methyl derivative (**20**) which appeared to have no effect on this process.

The newer derivatives (**23**, **24**) also significantly inhibited both invasion and attachment at 20 μM (data not shown). Wishing to find an endpoint of invasion inhibitory activity, we tested nostodione A and the entire mini-panel of structural analogues at 5 μM. Surprisingly, all of the derivative except **21** showed significant inhibition of tachyzoite host cell invasion at this lower concentration. Parent compound nostodione A (**1**) no longer showed such capacity. However, we found that attachment was no longer affected by compounds **1**, **17**–**20**, and **22** whereas the new derivatives **23** and **24** continued to display significant levels of attachment inhibition.

Interestingly, compound **21** distinguished itself by an apparent ability to enhance tachyzoite attachment. Such activity could be due to an effect on the secretion and/or processing of tachyzoite adhesins required for host cell attach-

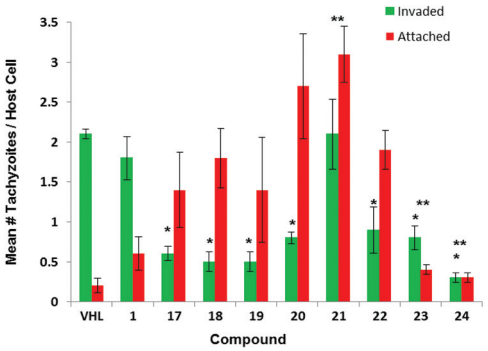

Fig. 6 Quantification of invasion inhibition by nostodione A and mini panel using red/green assay. Compounds (5 μM) were tested for activity directly on extracellular tachyzoites using an established method.[15b] Green bars represent invaded/intracellular parasites; red bars depict attached/extracellular parasites. Data are mean values ± SEM of three independent experiments. *Tachyzoite invasion was significantly reduced ($P \leq 0.05$, two-tailed Student's *t*-test) relative to VHL control. ** Tachyzoite attachment to host cell was significantly affected ($P \leq 0.05$, two-tailed Student's *t*-test) relative to VHL control.

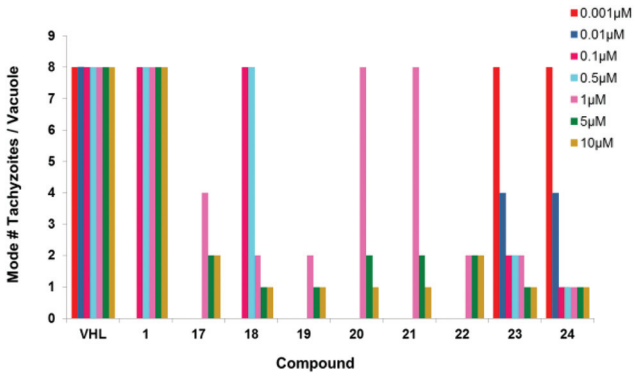

Fig. 7 Titration of replication inhibition by nostodione A and mini-panel of analogues. HFF monolayers were inoculated with tachyzoites and then incubated for 2 h at 37 °C/5% CO_2 thereby establishing an intracellular infection. Compounds or DMSO (vehicle; VHL) were added at the concentrations shown. Parasite replication proceeded for 26 h at which time the cells were fixed, permeabilized and immunolabeled. Data were compiled from three independent experiments and are expressed as the mode number of parasites per vacuole.

ment,[15d] a possibility that we are further investigating. We note from a structural viewpoint that **21** is the only derivative containing a meta-substituted aryl substituent, a feature that may be co-related to this activity.

Finally, we interrogated the mini panel for the ability to inhibit an established tachyzoite infection of the host cells using an established fluorescence-based replication assay.[15b] Based on the finding of robust invasion inhibition at relatively low concentrations, we performed a titration (**17**, **19–22** range = 1–10 μM; **1**, **18** range = 100 nM–10 μM; **23**, **24** range = 1 nM–10 μM) replication assay. *T. gondii* tachyzoites primarily replicate *via* endodyogeny in the host cell cytoplasm inside the protected environment of the parasitophorous vacuole. During one cycle of replication (6–8 hours) two daughter cells develop within and then destroy the one mother cell.[15c] Thus 2, 4, 8 tachyzoites within the vacuole represent 1, 2 and 3 cycles, respectively, of replication. A decrease in the number of intravacuolar tachyzoites relative to VHL indicates inhibition of intracellular replication. As shown in Fig. 7 nostodione A had no effect while all of the analogues effectively limited tachyzoite replication to ≤1 cycle at both 10 and 5 μM. As suggested in the invasion assay, **23** and **24** exhibited the largest dynamic range of inhibitory ability effectively limiting replication to ≤1 cycle at 100 nM concentration and just 2 cycles at 10 nM.

In conclusion, we report the full details on our total synthesis of the cyanobacterial natural product nostodione A in 8 chemical steps and 21.6% overall yield from commercially available ethyl indole-2-carboxylate.[16] A crystal structure on analog **19** firmly establishes the 1,2-dicarbonyl structure within an extended H-bonded network. The synthetic strategy employed a diversity-oriented late stage Horner–Wadsworth–Emmons olefination allowing for the assembly of a mini-panel of structural analogues. Further details of the antiparasitic biological activity of nostodione A were established taking advantage of this diversity-oriented synthetic paradigm. The trifluoromethoxyaryl derivative **23** and more significantly the trifuoromethoxy-diarylether functionalised analogue **24** proved to have potent and promising activity against *in vitro T. gondii* tachyzoites. Overall, this work has permitted the discovery of a valuable lead anti-Toxoplasma pharmacophore through incorporation of a 4-aryloxy substituent on the nostodione A phenolic substituent. These preliminary results also indicate interesting diversity in the structure–activity relationships (SAR) of the compounds relevant to the inhibition or enhancement of host cell attachment and invasion by *T. gondii* tachyzoites and inhibition of intracellular tachyzoite replication. Further *in vitro* biological studies to delineate the mechanism of such SARs in more detail are in progress. In conclusion, these data indicate that nostodione A derivative **24** can prevent as well as treat *in vitro T. gondii* infection and thus represents a viable candidate for examination *in vivo* against a mouse model of acute and chronic toxoplasmosis.

Experimental

Ethyl 1-tosyl-1*H*-indole-2-carboxylate (8)

Into a flame-dried flask with a stirring bar was added ethyl indole-2-carboxylate (1.0 g, 1.0 equiv., 5.28 mmol). Dimethylformamide (8.0 mL) was added to the flask under an inert atmosphere. Sodium hydride (0.32 g, 1.5 equiv., 60% dispersion in mineral oil) was added to the flask in portions while maintaining the temperature at 0 °C. The reaction mixture was stirred for 30 min at 0 °C. 4-Toluenesulfonyl chloride (2.01 g, 2.0 equiv., 10.5 mol) was added to the flask slowly in portions. The reaction mixture was stirred for 30 min at

0 °C and then overnight (12 h) at room temperature. Reaction mixture was diluted with excess water and extracted with ethyl acetate (3 × 100 mL). The organic layer was washed with brine and dried over sodium sulfate to give crude product which was purified using silica-gel flash chromatography (10–15% of EtOAc : hexanes, gradient elution) to yield ethyl 1-tosyl-1*H*-indole-2-carboxylate. Yield = 93%. ^{1}H NMR (600 MHz, $CDCl_3$) δ 8.13 (d, J = 8.5 Hz, 1H), 7.95 (d, J = 8.4 Hz, 2H), 7.58 (d, J = 7.8 Hz, 1H), 7.45 (ddd, J = 8.4, 7.3, 1.1 Hz, 1H), 7.32–7.25 (m, 3H), 7.17 (s, 1H), 4.44 (q, J = 7.1 Hz, 2H), 2.39 (s, 3H), 1.42 (t, J = 7.2 Hz, 3H). ^{13}C NMR (151 MHz, $CDCl_3$) δ 161.51, 145.02, 138.26, 135.82, 132.04, 129.66, 128.36, 127.52, 127.04, 124.16, 122.55, 116.60, 115.51, 62.06, 21.74, 14.25.

(1-Tosyl-1*H*-indol-2-yl)methanol (9)

Into a flame-dried flask with a stirring bar was added ethyl 1-tosyl-1*H*-indole-2-carboxylate (1.0 g, 1.0 equiv., 2.91 mmol). Dichloromethane (8.00 mL) was added to the flask under inert atmosphere. The reaction mixture was cooled to −78 °C whereupon; DIBAL (7.28 mL, 2.5 equiv., 1 M solution in cyclohexane) was added drop wise to the flask. The reaction mixture was stirred at −78 °C for additional 2 h. The reaction mixture was then allowed to warm to room temperature and stirred overnight (12 h). The reaction mixture was diluted with diethyl ether and cooled to 0 °C. Slowly water (0.30 mL) was added to the reaction mixture followed by 15% aqueous sodium hydroxide (0.30 mL). Additional water (0.72 mL) was added and then allowed the reaction mixture to warm to room temperature and stir for 15 minutes. Anhydrous magnesium sulphate was added to the flask and further reaction mixture was stirred for 15 minutes. The reaction mixture was filtered and washed with dichloromethane to remove salts. The filtrate was concentrated to give crude product which was purified using silica-gel flash chromatography (15–30% of EtOAc : hexanes, gradient elution) to yield (1-tosyl-1*H*-indol-2-yl)methanol.[16b] Yield = 96%. ^{1}H NMR (600 MHz, $CDCl_3$) δ 8.05 (d, J = 8.4 Hz, 1H), 7.71 (d, J = 8.4 Hz, 2H), 7.48 (d, J = 7.7 Hz, 1H), 7.32–7.28 (m, 1H), 7.23 (t, J = 7.5 Hz, 1H), 7.20 (d, J = 8.3 Hz, 2H), 6.64 (s, 1H), 4.91 (s, 2H), 3.31 (brs, 1H), 2.33 (s, 3H). ^{13}C NMR (151 MHz, $CDCl_3$) δ 145.25, 140.31, 137.09, 135.64, 130.06, 129.21, 126.51, 125.06, 123.83, 121.28, 114.45, 111.28, 58.67, 21.63.

2-(Chloromethyl)-1-tosyl-1*H*-indole (10)

Into a flame-dried flask with a stirring bar was added (1-tosyl-1*H*-indol-2-yl)methanol (1.0 g, 1.0 equiv., 3.31 mmol). Dichloromethane (8.00 mL) was added to the flask under an inert atmosphere. The reaction mixture was cooled to 0 °C. Triphenylphosphine (1.74 g, 2.0 equiv., 6.63 mmol) was added to the flask. *N*-Chlorosuccinimide (0.755 g, 1.7 equiv., 5.64 mmol) was then added slowly to the flask at 0 °C. (The reaction was monitored by using TLC). The reaction mixture was stirred approximately for 20 min at 0 °C. Upon completion of reaction, the reaction mixture was diluted with water and extracted with ethyl acetate (3 × 100 mL). The organic layer was washed with brine and dried over sodium sulfate to give crude product which was purified using silica-gel flash chromatography (10–15% of EtOAc : hexanes, gradient elution) to yield 2-(chloromethyl)-1-tosyl-1*H*-indole. Yield = 92%. M.P.: 53–55 °C. ^{1}H NMR (600 MHz, $CDCl_3$) δ 8.00 (dd, J = 8.5, 0.7 Hz, 1H), 7.69 (d, J = 8.4 Hz, 2H), 7.40 (d, J = 7.8 Hz, 1H), 7.24 (ddd, J = 8.5, 7.3, 1.2 Hz, 1H), 7.18–7.14 (m, 1H), 7.12 (d, J = 8.1 Hz, 2H), 6.71 (d, J = 0.5 Hz, 1H), 4.99 (s, 2H), 2.25 (s, 3H). ^{13}C NMR (151 MHz, $CDCl_3$) δ 145.25, 137.35, 136.49, 135.75, 129.96, 128.83, 126.91, 125.53, 123.93, 121.37, 114.83, 113.12, 39.05, 21.69. HRMS: calcd For $C_{16}H_{14}ClNO_2S$ $[M]^+$ 319.0430; found 319.0434.

Dimethyl (1-tosyl-1*H*-indol-2-yl)methylphosphonate (11)

Into a 10–20 mL Biotage microwave vial with a stirring bar was added 2-(chloromethyl)-1-tosyl-1*H*-indole (1.0 g, 1.0 equiv., 3.12 mmol). Trimethyl phosphite (1.94 mL, 5 equiv., 15.6 mmol) was added to the vial. The reaction mixture was sealed and heated to 100 °C overnight (12 h). The reaction mixture was diluted with water and extracted with ethyl acetate (3 × 100 mL). The organic layer was washed with brine and dried over sodium sulfate. The solvent was removed using rotary evaporator (*caution! Use proper ventilation*.) to give crude product which was purified using silica-gel flash chromatography (50–90% of EtOAc : hexanes, gradient elution) to yield dimethyl (1-tosyl-1*H*-indol-2-yl)methylphosphonate. Yield = 92%. ^{1}H NMR (600 MHz, $CDCl_3$) δ 8.10 (d, J = 8.4 Hz, 1H), 7.62 (d, J = 8.4 Hz, 2H), 7.43 (d, J = 7.7 Hz, 1H), 7.27 (t, J = 7.7 Hz, 1H), 7.23–7.19 (m, 1H), 7.17 (d, J = 8.1 Hz, 2H), 6.81 (d, J = 3.5 Hz, 1H), 3.81–3.76 (m, 2H), 3.77 (s, 3H), 3.75 (s, 3H), 2.31 (s, 3H). ^{13}C NMR (151 MHz, $CDCl_3$) δ 145.10, 137.10, 135.69, 130.82 (d, J = 5.7 Hz), 129.96, 129.66, 126.51, 124.65, 123.94, 120.78, 115.15, 112.73 (d, J = 6.8 Hz), 53.24, 53.20, 25.42 (d, J = 142.8 Hz), 21.64. ^{31}P NMR (243 MHz, $CDCl_3$) δ 26.50. HRMS: calcd For $C_{18}H_{20}NO_5PS$ $[M]^+$ 393.0795; found 393.0800.

Dimethyl (1*H*-indol-2-yl)methylphosphonate (12)

Into a flame-dried flask with a stirring bar was added dimethyl (1-tosyl-1*H*-indol-2-yl)methylphosphonate (0.200 g, 1.0 equiv., 0.50 mmol). THF (5.0 mL) was added to the flask under inert atmosphere. The reaction mixture was cooled to 0 °C. Tetra-*n*-butylammonium fluoride (4.06 mL, 8.0 equiv., 4.06 mmol, 1 M solution in THF) was added drop wise to the flask. The reaction mixture was then allowed to warm to room temperature and stirred overnight (15 h). The reaction mixture was diluted with excess water and extracted with ethyl acetate (3 × 50 mL). The organic layer was washed with brine and dried over sodium sulfate and evaporated using rotary evaporator to give crude product which was purified using silica-gel flash chromatography (0–3% of MeOH : DCM, gradient elution) to yield dimethyl (1*H*-indol-2-yl)methylphosphonate. Yield = 76%. M.P.: 112–114 °C. ^{1}H NMR (600 MHz, $CDCl_3$) δ 8.97 (s, 1H), 7.54 (d, J = 7.8 Hz, 1H), 7.34 (dd, J = 8.1, 0.6 Hz, 1H), 7.15 (t, J = 7.6 Hz, 1H), 7.10–7.06 (m, 1H), 6.36 (s, 1H), 3.72 (s, 3H), 3.70 (s, 3H), 3.37 (d, J = 20.9 Hz, 2H). ^{13}C NMR (151 MHz, $CDCl_3$) δ 136.59, 128.44, 128.03 (d, J = 10.5 Hz), 121.93, 120.12, 119.98, 111.09, 102.69 (d, J = 10.7 Hz), 53.35, 53.31, 25.66

(d, J = 140.6 Hz).^{31}P NMR (243 MHz, $CDCl_3$) δ 27.24. HRMS: calcd For $C_{11}H_{14}NO_3P$ $[M]^+$ 239.0714; found 239.0711.

Methyl 2-(2-((dimethoxyphosphoryl)methyl)-1*H*-indol-3-yl)-2-oxoacetate (14)

Into a flame-dried flask with a stirring bar was added dimethyl (1*H*-indol-2-yl)methylphosphonate (0.053 g, 1.0 equiv., 0.22 mmol). Freshly distilled diethyl ether (20.0 mL) was added to the flask under inert atmosphere. The reaction mixture was sonicated for 5 min and then cooled to 0 °C. Oxalyl chloride (0.047 mL, 2.5 equiv., 0.55 mmol) was added drop wise to the flask. The reaction mixture was stirred at 0 °C for additional 2.0 h. Methanol (excess) was added to the flask and then the reaction mixture was then allowed to warm to room temperature and stirred for additional 2.0 h. Diethyl ether was removed under reduced pressure and the crude reaction mixture was purified using silica-gel flash chromatography (0–4% of MeOH : DCM, gradient elution) to yield methyl 2-(2-((dimethoxyphosphoryl)methyl)-1*H*-indol-3-yl)-2-oxoacetate. Yield = 92%. ^{1}H NMR (600 MHz, $CDCl_3$) δ 10.82 (s, 1H), 7.67 (d, J = 8.0 Hz, 1H), 7.24–7.22 (m, 1H), 7.21–7.19 (m, 1H), 7.18–7.14 (m, 1H), 4.02 (s, 3H), 3.99 (d, J = 21.7 Hz, 2H), 3.79 (s, 3H), 3.77 (s, 3H). ^{13}C NMR (151 MHz, $CDCl_3$) δ 181.92, 166.14, 139.60 (d, J = 9.6 Hz), 135.59, 125.86, 123.85, 123.04, 119.61, 112.08, 110.39, 53.65, 53.60, 52.84, 24.49 (d, J = 136.8 Hz). ^{31}P NMR (243 MHz, $CDCl_3$) δ 26.14. HRMS: calcd For $C_{14}H_{16}NO_6P$ $[M]^+$ 325.0715; found 325.0711.

Dimethyl 1,2-dioxo-1,2,3,4-tetrahydrocyclopenta[*b*]indol-3-ylphosphonate (15)

Into a flame-dried two necked round bottom flask with a stirring bar and a reflux condenser was added methyl 2-(2-((dimethoxyphosphoryl)methyl)-1*H*-indol-3-yl)-2-oxoacetate (0.105 g, 1.0 equiv., 0.32 mmol). Freshly distilled THF (40.0 mL) was added to the flask under inert atmosphere. The reaction mixture was cooled to 0 °C. Sodium hydride (0.031 g, 2.5 equiv., 0.80 mmol, 60% dispersion in mineral oil) was added to the flask. The reaction mixture was heated at reflux approximately 12 h (overnight, check TLC) in oil bath. During this time the solution develops an intense red color. Excess THF was distilled off under reduced pressure and the crude reaction mixture was purified using silica-gel flash chromatography [2–15% of MeOH : DCM, gradient elution (very slow column)] to yield dimethyl 1,2-dioxo-1,2,3,4-tetrahydro-cyclopenta[*b*]indol-3-ylphosphonate. Yield = 55–60%. ^{1}H NMR (600 MHz, DMSO) δ 12.98 (s, 1H), 7.84 (d, J = 7.7 Hz, 1H), 7.64 (d, J = 8.1 Hz, 1H), 7.42 (t, J = 7.6 Hz, 1H), 7.34 (t, J = 7.3 Hz, 1H), 5.01 (d, J = 26.4 Hz, 1H), 3.79 (d, J = 11.2 Hz, 3H), 3.70 (d, J = 11.1 Hz, 3H). ^{13}C NMR (151 MHz, DMSO) δ 194.79, 175.44, 158.57 (d, J = 9.0 Hz), 140.09, 125.61, 123.62, 123.07 (d, J = 5.6 Hz), 120.92, 120.65, 113.72, 53.76 (d, J = 6.1 Hz), 53.56 (d, J = 6.5 Hz), 43.93 (d, J = 136.6 Hz). ^{31}P NMR (243 MHz, DMSO) δ 17.00. HRMS (ES): calcd For $C_{13}H_{13}NO_5P$ $[M]^+$ 294.0525; found 294.0531.

Nostodione A (1)

Into a flame-dried two necked round bottom flask with a stirring bar and a reflux condenser was added dimethyl 1,2-dioxo-1,2,3,4-tetrahydrocyclopenta[*b*]indol-3-ylphosphonate (0.034 g, 1.0 equiv., 0.11 mmol). DMF (3.5 mL) was added to the flask under inert atmosphere. The reaction mixture was cooled to 0 °C. Sodium hydride (0.012 g, 2.5 equiv., 0.29 mmol, 60% dispersion in mineral oil) was added to the flask. The reaction mixture was stirred for 5 min at 0 °C. 4-(Tetrahydro-2*H*-pyran-2-yloxy)benzaldehyde (0.048 g, 2 equiv., 0.23 mmol) was added to the flask. The reaction mixture was then heated at reflux approximately 12 h (overnight) in oil bath. Excess DMF was distilled off under vacuum. The crude reaction mixture was dissolved in dichloromethane and passed through a short packed silica gel bed. Dichloromethane was evaporated under reduced pressure. The crude material was re-dissolved in dry MeOH (5.0 mL) and *p*-toluenesulphonic acid (10 mol%) was added to the flask. The reaction mixture was refluxed for 30 minutes. Methanol was evaporated under reduced pressure and the crude reaction mixture was purified using silica-gel flash chromatography (0–5% of MeOH : DCM, gradient elution) to yield nostodione A (**1**).[6b] Yield = 68%. M.P.: decompose at >285 °C. ^{1}H NMR (600 MHz, DMSO, Major isomer) δ 12.21 (s, 1H), 10.26 (br s, 1H), 7.83 (d, J = 7.8 Hz, 1H), 7.73 (d, J = 8.2 Hz, 2H), 7.66 (d, J = 8.1 Hz, 1H), 7.41 (ddd, J = 8.1, 7.2, 0.9), 7.33 (ddd, J = 8.1, 7.2, 0.9), 7.29 (s, 1H), 6.96 (d, J = 8.6 Hz, 2H). ^{13}C NMR (151 MHz, DMSO) δ 193.60, 176.93, 159.85, 158.91, 141.25/140.77, 131.86, 128.71, 126.34, 124.59, 123.84, 123.80, 121.01, 120.74, 119.41/119.06, 116.42, 114.34. ^{1}H NMR (600 MHz, DMSO, Minor isomer) δ 12.93 (s, 1H), 10.35 (s, 1H), 8.08 (d, J = 8.7 Hz, 2H), 7.76 (d, J = 7.8 Hz, 1H), 7.57 (d, J = 8.1 Hz, 1H), 7.38 (ddd, J = 8.2, 7.2, 1.1), 7.29 (ddd, J = 8.0, 7.1, 0.8), 7.23 (s, 1H), 6.90 (d, J = 8.7 Hz, 2H). ^{13}C NMR (151 MHz, DMSO) δ 192.53, 175.98, 164.56, 160.47, 141.25/140.77, 134.07, 131.91, 126.01, 125.25, 123.60, 121.65, 121.08, 119.66, 119.41/119.06, 115.70, 113.17. HRMS: calcd For $C_{18}H_{11}NO_3$ $[M]^+$ 289.0731; found 289.0739.

3-(4-Chlorobenzylidene)cyclopenta[*b*]indole-1,2(3*H*,4*H*)-dione (17)

Isomeric ratio: 83 : 17. M.P.: decomposes at >290 °C. Major isomer: ^{1}H NMR (600 MHz, DMSO) δ 12.20 (s, 1H), 7.87 (d, J = 7.8 Hz, 1H), 7.82 (d, J = 8.3 Hz, 2H), 7.65 (d, J = 8.3 Hz, 1H), 7.63 (d, J = 8.5 Hz, 2H), 7.47–7.43 (m, 1H), 7.38 (s, 1H), 7.37–7.33 (m, 1H). Minor isomer: ^{1}H NMR (600 MHz, DMSO) δ 13.08 (s, 1H), 8.08 (d, J = 8.6 Hz, 2H), 7.82 (d, J = 8.3 Hz, 1H, overlap with major isomer), 7.63 (d, J = 8.5 Hz, 1H, overlap with major isomer), 7.57 (d, J = 8.6 Hz, 2H), 7.45–7.42 (m, 1H), 7.34–7.31 (m, 1H), 7.29 (s, 1H). ^{13}C NMR (151 MHz, DMSO) δ 193.01 (major), 192.28 (minor), 176.90 (major), 175.96 (minor), 162.77, 157.33, 140.89, 140.86, 135.01, 134.53, 132.84 (minor), 132.76, 132.42, 130.96 (major), 129.52 (major), 129.00 (minor), 128.63 (minor), 127.02 (major), 126.71 (minor), 126.37 (major), 125.35, 124.06 (major), 123.79 (minor), 123.08, 121.43 (minor), 121.34, 121.06 (major), 120.70, 114.19 (major),

113.40 (minor). HRMS: calcd For $C_{18}H_{10}ClNO_2$ $[M]^+$ 307.0403; found 307.0400.

3-(4-(Benzyloxy)benzylidene)cyclopenta[*b*]indole-1,2-(3*H*,4*H*)-dione (18)

Isomeric ratio: 94 : 06. M.P.: decomposes at >247 °C. Major isomer: ^{1}H NMR (600 MHz, DMSO) δ 12.25 (s, 1H), 7.85 (d, J = 7.8 Hz, 1H), 7.79 (d, J = 8.6 Hz, 2H), 7.66 (d, J = 8.2 Hz, 1H), 7.50 (d, J = 7.3 Hz, 2H), 7.45–7.42 (m, 2H), 7.44–7.40 (m, 1H), 7.38–7.35 (m, 1H), 7.34 (s, 1H), 7.33–7.32 (m, 1H), 7.22 (d, J = 8.6 Hz, 2H), 5.23 (s, 2H). Major isomer: ^{13}C NMR (151 MHz, DMSO) δ 193.24, 177.01, 160.09, 158.16, 140.73, 136.66, 131.47, 128.53, 128.14, 128.03, 127.81, 126.60, 126.32, 124.15, 123.98, 120.84, 120.80, 120.43, 115.80, 114.16, 69.51. HRMS: calcd For $C_{25}H_{17}NO_3$ $[M]^+$ 379.1203; found 379.1208.

3-(4-Methoxybenzylidene)cyclopenta[*b*]indole-1,2(3*H*,4*H*)-dione (19)

Isomeric ratio: 94 : 06. M.P.: decomposes with melt at 290–294 °C. Major isomer: ^{1}H NMR (600 MHz, DMSO) δ 12.22 (s, 1H), 7.84 (d, J = 7.8 Hz, 1H), 7.79 (d, J = 8.6 Hz, 2H), 7.66 (d, J = 8.2 Hz, 1H), 7.44–7.39 (m, 1H), 7.34–7.31 (m, 2H) *including the olefinic -H*, 7.14 (d, J = 8.8 Hz, 2H), 3.88 (s, 3H). ^{13}C NMR (151 MHz, DMSO) δ 193.27, 176.99, 160.97, 158.24, 140.80, 131.44, 128.17, 126.56, 126.13, 124.12, 123.94, 120.81, 120.41, 115.01, 114.17, 55.47. HRMS: calcd For $C_{19}H_{13}NO_3$ $[M]^+$ 303.0907; found 303.0895.

3-(4-Methylbenzylidene)cyclopenta[*b*]indole-1,2(3*H*,4*H*)-dione (20)

Isomeric ratio: 88 : 12. M.P.: decomposes with melt >308–310 °C. Major isomer: ^{1}H NMR (600 MHz, DMSO) δ 12.20 (s, 1H), 7.85 (d, J = 7.8 Hz, 1H), 7.70 (d, J = 8.0 Hz, 2H), 7.67 (d, J = 8.2 Hz, 1H), 7.45–7.41 (m, 1H), 7.39 (d, J = 7.9 Hz, 2H), 7.36–7.32 (m, 2H) *including the olefinic -H*, 3.33 (s, 1H). ^{13}C NMR (151 MHz, DMSO) δ 193.19, 176.95, 157.78, 140.78, 140.21, 130.94, 130.10, 129.35, 128.07, 126.74, 124.69, 123.98, 121.63, 120.91, 120.73, 114.24, 21.18. HRMS: calcd For $C_{19}H_{13}NO_2$ $[M]^+$ 287.0946; found 287.0946.

3-(Benzo[*d*][1,3]dioxol-5-ylmethylene)cyclopenta[*b*]indole-1,2(3*H*,4*H*)-dione (21)

Isomeric ratio: 95 : 05. M.P.: decomposes with melt >320 °C. Major isomer: ^{1}H NMR (600 MHz, DMSO) δ 12.25 (s, 1H), 7.84 (d, J = 7.8 Hz, 1H), 7.66 (d, J = 8.2 Hz, 1H), 7.42 (t, J = 7.7 Hz, 1H), 7.38–7.35 (m, 2H), 7.33 (t, J = 7.5 Hz, 1H), 7.30 (s, 1H), 7.11 (d, J = 7.9 Hz, 1H), 6.16 (s, 2H). ^{13}C NMR (151 MHz, DMSO) δ 193.21, 176.94, 158.09, 149.21, 148.06, 140.82, 128.18, 127.78, 126.64, 124.96, 124.35, 123.95, 120.97, 120.87, 120.81, 114.15, 109.31, 108.92, 101.80. HRMS: calcd For $C_{19}H_{11}NO_4$ $[M]^+$ 317.0685; found 317.0688.

3-(4-Nitrobenzylidene)cyclopenta[*b*]indole-1,2(3*H*,4*H*)-dione (22)

Isomeric ratio: >98 : 02. M.P.: decomposes with melt >300 °C. Major isomer: ^{1}H NMR (600 MHz, DMSO) δ 12.21 (s, 1H), 8.39 (d, J = 8.7 Hz, 2H), 8.05 (d, J = 8.6 Hz, 2H), 7.90 (d, J = 7.8 Hz, 1H), 7.65 (d, J = 8.2 Hz, 1H), 7.50–7.44 (m, 2H)) *including the olefinic -H*, 7.36 (t, J = 7.6 Hz, 1H). ^{13}C NMR (151 MHz, DMSO) δ 192.81, 176.83, 156.77, 147.54, 141.24, 140.83, 130.31, 127.41, 126.46, 125.28, 124.68, 124.48, 124.14, 123.48, 121.26, 120.68, 114.28. HRMS: calcd For $C_{18}H_{10}N_2O_4$ $[M]^+$ 318.0645; found 318.0641.

3-(4-(4-(Trifluoromethoxy)phenoxy)benzylidene)cyclo-penta[*b*]-indole-1,2(3*H*,4*H*)-dione (23)

Isomeric ratio: 95 : 05. M.P.: 350–355 °C. Major isomer: ^{1}H NMR (600 MHz, DMSO) δ 12.27 (s, 1H), 7.92 (d, J = 8.6 Hz, 2H), 7.86 (d, J = 7.8 Hz, 1H), 7.65 (d, J = 8.2 Hz, 1H), 7.53 (d, J = 8.3 Hz, 2H), 7.44 (t, J = 7.7 Hz, 1H), 7.38 (s, 1H), 7.34 (t, J = 7.5 Hz, 1H). ^{13}C NMR (151 MHz, DMSO) δ 193.00, 176.86, 157.19, 149.12, 140.91, 133.00, 131.37, 127.05, 126.01, 125.52, 124.06, 123.11, 121.69, 121.09, 120.70, 120.08 (q, J = 257.31 Hz), 114.19. HRMS (EI$^+$): calcd For $C_{19}H_{10}F_3NO_3$ $[M]^+$ 357.0617; found 357.0613.

3-(4-(Trifluoromethoxy)benzylidene)cyclopenta[*b*]indole-1,2(3*H*,4*H*)-dione (24)

Isomeric ratio: 90 : 10. M.P.: decomposes with melt at 305–310 °C. Major isomer: ^{1}H NMR (700 MHz, DMSO) δ 12.21 (s, 1H), 7.87–7.83 (m, 3H), 7.65 (d, J = 8.2 Hz, 1H), 7.48 (d, J = 8.6 Hz, 2H), 7.44–7.41 (m, 1H), 7.36 (s, 1H), 7.35–7.31 (m, 1H), 7.28 (d, J = 9.0 Hz, 2H), 7.18 (d, J = 8.6 Hz, 2H). ^{13}C NMR (176 MHz, DMSO) δ 193.17, 176.92, 158.12, 157.75, 154.41, 144.40, 140.84, 131.65, 129.04, 127.24, 126.78, 124.77, 124.00, 123.20, 121.61, 121.10, 120.94, 120.76, 120.11(q, J = 256 Hz), 118.87, 114.19. HRMS (EI$^+$): calcd For $C_{25}H_{14}F_3NO_4$ $[M]^+$ 449.0850; found 449.0875.

Acknowledgements

We thank NSERC (JMcN, KK) and the Stanley Medical Research Institute (CB, RY, LJB, JMcN) for financial support of this work.

Notes and references

1 A. M. Burja, B. Banaigs, E. Abou-Mansour, J. G. Burgess and P. C. Wright, *Tetrahedron*, 2001, **57**, 9347.
2 A. Kobayashi, S. Kajiyama, K. Inawaka, H. Kanzaki and K. Kawazu, *Z. Naturforsch., C: Biosci.*, 1994, **49**, 464.
3 S. S. Hee, G. Chlipala and J. Orjala, *J. Microbiol. Biotechnol.*, 2008, **18**, 1655.
4 (*a*) A. Ploutno and S. Carmeli, *J. Nat. Prod.*, 2001, **64**, 544; (*b*) E. P. Balskus and C. T. Walsh, *J. Am. Chem. Soc.*, 2009, **131**, 14648.
5 P. J. Proteau, W. H. Gerwick, F. Garcia-Pichel and R. Castenholz, *Experientia*, 1993, **49**, 825.
6 (*a*) J. C. Badenock, J. J. Jordan and G. W. Gribble, *Tetrahedron Lett.*, 2013, **54**, 2759; (*b*) A. Ekebergh, A. Börje and

J. Mårtensson, *Org. Lett.*, 2012, **14**, 6274; (*c*) A. Ekebergh, I. Karlsson, R. Mete, Y. Pan, A. Börje and J. Mårtensson, *Org. Lett.*, 2011, **13**, 4458; (*d*) S. Malla and M. O. A. Sommer, *Green Chem.*, 2014, **16**, 3255; (*e*) A. Ekebergh, C. Lingblom, P. Sandin, C. Wennerås and J. Mårtensson, *Org. Biomol. Chem.*, 2015, **13**, 3382; (*f*) J. McNulty, K. Keskar, C. Bordón, R. Yolken and L. Jones-Brando, *Chem. Commun.*, 2014, **50**, 8904.

7 J. McNulty, R. Vemula, C. Bordón, R. Yolken and L. Jones-Brando, *Org. Biomol. Chem.*, 2014, **12**, 255.

8 B. Krivogorsky, P. Grundt, R. Yolken and L. Jones-Brando, *Antimicrob. Agents Chemother.*, 2008, **52**, 4466.

9 R. A. Davis, M. S. Buchanan, S. Duffy, V. M. Avery, S. A. Charman, W. N. Charman, K. L. White, D. M. Shackleford, M. D. Edstein, K. T. Andrews, D. Camp and R. J. Quinn, *J. Med. Chem.*, 2012, **55**, 5851.

10 (*a*) K. M. Maloney and J. Y. L. Chung, *J. Org. Chem.*, 2009, **74**, 7574; (*b*) T. Maegawa, K. Otake, K. Hirosawa, A. Goto and H. Fujioka, *Org. Lett.*, 2012, **14**, 4798; (*c*) A. Samarat, V. Fargeas, J. Villières, J. Lebreton and H. Amri, *Tetrahedron Lett.*, 2001, **42**, 1273.

11 (*a*) A. Yasuhara and T. Sakamoto, *Tetrahedron Lett.*, 1998, **39**, 595; (*b*) S. K. Jackson and M. A. Kerr, *J. Org. Chem.*, 2007, **72**, 1405; (*c*) S. Krishnan, J. T. Bagdanoff, D. C. Ebner, Y. K. Ramtohul, U. K. Tambar and B. M. Stoltz, *J. Am. Chem. Soc.*, 2008, **130**, 13745.

12 (*a*) All derivatives of nostodione A were isolated as amorphous pigments and resisted attempts at crystallization form various solvents. An NMR sample of nostodione A methyl ether (**19**) in $(CD_3)_2SO$ was observed to slowly deposit crystals that proved suitable for X-ray analysis. The structure data for nostodione methylether are depositied under CCDC 1051478; (*b*) M. J. Frisch, G. W. Trucks, H. B. Schlegel, G. E. Scuseria, M. A. Robb, J. R. Cheeseman, G. Scalmani, V. Barone, B. Mennucci, G. A. Petersson, H. Nakatsuji, M. Caricato, X. Li, H. P. Hratchian, A. F. Izmaylov, J. Bloino, G. Zheng, J. L. Sonnenberg, M. Hada, M. Ehara, K. Toyota, R. Fukuda, J. Hasegawa, M. Ishida, T. Nakajima, Y. Honda, O. Kitao, H. Nakai, T. Vreven, J. A. Montgomery Jr., J. E. Peralta, F. Ogliaro, M. Bearpark, J. J. Heyd, E. Brothers, K. N. Kudin, V. N. Staroverov, T. Keith, R. Kobayashi, J. Normand, K. Raghavachari, A. Rendell, J. C. Burant, S. S. Iyengar, J. Tomasi, M. Cossi, N. Rega, J. M. Millam, M. Klene, J. E. Knox, J. B. Cross, V. Bakken, C. Adamo, J. Jaramillo, R. Gomperts, R. E. Stratmann, O. Yazyev, A. J. Austin, R. Cammi, C. Pomelli, J. W. Ochterski, R. L. Martin, K. Morokuma, V. G. Zakrzewski, G. A. Voth, P. Salvador, J. J. Dannenberg, S. Dapprich, A. D. Daniels, O. Farkas, J. B. Foresman, J. V. Ortiz, J. Cioslowski and D. J. Fox, *Gaussian 09, Revision C.01*, Gaussian, Inc., Wallingford CT, 2010.

13 (*a*) A. Nilsen, G. P. Miley, I. P. Forquer, M. W. Mather, K. Katneni, Y. Li, S. Pou, A. M. Pershing, A. M. Stickles, E. Ryan, J. X. Kelly, J. S. Doggett, K. L. White, D. J. Hinrichs, R. W. Winter, S. A. Charman, L. N. Zakharov, I. Bathurst, J. N. Burrows, A. B. Vaidya and M. K. Riscoe, *J. Med. Chem.*, 2014, **57**, 3818; (*b*) C. L. Yeates, J. F. Batchelor, E. C. Capon, N. J. Cheesman, M. Fry, A. T. Hudson, M. Pudney, H. Trimming, J. Woolven, J. M. Bueno, J. Chicharro, E. Fernández, J. M. Fiandor, D. Gargallo-Viola, F. Gómez de las Heras, E. Herreros and M. L. León, *J. Med. Chem.*, 2008, **51**, 2845; (*c*) J. S. Doggett, A. Nilsen, I. Forquer, K. W. Wegmann, L. Jones-Brando, R. H. Yolken, C. Bordón, S. A. Charman, K. Katneni, T. Schultz, J. N. Burrows, D. J. Hinrichs, B. Meunier, V. B. Carruthers and M. K. Riscoe, *Proc. Natl. Acad. Sci. U. S. A.*, 2012, **109**, 15936.

14 P. Das, X. Deng, L. Zhang, M. G. Roth, B. M. A. Fontoura, M. A. Philips and J. K. De Brabander, *ACS Med. Chem. Lett.*, 2013, **4**, 517.

15 (*a*) L. Jones-Brando, E. F. Torrey and R. Yolken, *Schizophr. Res.*, 2003, **62**, 237; (*b*) C. P. Hencken, L. Jones-Brando, C. Bordón, R. Stohler, B. T. Mott, R. Yolken, G. H. Posner and L. E. Woodard, *J. Med. Chem.*, 2010, **53**, 3594; (*c*) J. P. Dubey, D. S. Lindsay and C. A. Speer, *Clin. Microbiol. Rev.*, 1998, **11**, 267; (*d*) G. Rugarabamu, J. B. Marq, A. Guérin, M. Lebrun and D. Soldati-Favre, *Mol. Microbiol.*, 2015, **97**, 244.

16 (*a*) J. McNulty and K. Keskar, *Eur. J. Org. Chem.*, 2011, 6902; (*b*) J. McNulty and K. Keskar, *Eur. J. Org. Chem.*, 2014, 1622.

